HHS Public Access

Author manuscript

Langmuir. Author manuscript; available in PMC 2019 November 06.

Published in final edited form as:

Langmuir. 2018 November 06; 34(44): 13252–13262. doi:10.1021/acs.langmuir.8b01979.

Opto-Thermophoretic Attraction, Trapping, and Dynamic Manipulation of Lipid Vesicles

Eric H. Hill[1,2,*], **Jingang Li**[1], **Linhan Lin**[1], **Yaoran Liu**[1], and **Yuebing Zheng**[1,*]

[1]Texas Materials Institute; Department of Mechanical Engineering, The University of Texas at Austin, Austin, TX 78712, USA.

[2]Institute of Advanced Ceramics, Hamburg University of Technology, 21073 Hamburg, Germany

Abstract

Lipid vesicles are important biological assemblies which are critical to biological transport processes, and vesicles prepared in the lab are a workhorse for studies of drug delivery, protein unfolding, biomolecular interactions, compartmentalized chemistry, and stimuli-responsive sensing. Optical tweezers, the current method for holding lipid vesicles in place for single-vesicle studies, suffers from limitations such as high optical power, rigorous optics, and a small difference in the refractive indices of vesicles and water. Herein we report the use of plasmonic heating to trap vesicles in a temperature gradient, allowing long-range attraction, parallel trapping, and dynamic manipulation. The capabilities and limitations with respect to thermal effects on vesicle structure and optical spectroscopy are discussed. This simple approach allows vesicle manipulation using down to three orders of magnitude lower optical power and at least an order of magnitude higher trapping stiffness per unit power than traditional optical tweezers while using a simple optical setup. In addition to the benefit provided by the relaxation of these technical constraints, this technique can complement optical tweezers to allow detailed studies on thermophoresis of optically-trapped vesicles and effects of locally-generated thermal gradients on the physical properties of lipid vesicles. Finally, the technique itself and the large-scale collection of vesicles has huge potential for future studies of vesicles relevant to detection of exosomes, lipid raft formation, and other areas relevant to the life sciences.

Graphical Abstract

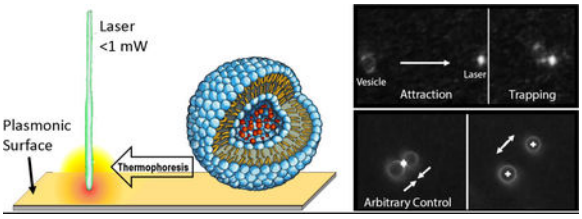

* eric.hill@tuhh.de, zheng@austin.utexas.edu.

Supporting Information

Measurements of ζ-potential and hydrodynamic radii of as-prepared DOPG vesicles; video snapshots of cationic DOTAP vesicle repulsion from the laser spot and of DOPG vesicle rupture at higher optical powers; videos of the dynamic manipulation, long-range vesicle collection, and vesicle rupture at higher optical powers.

Keywords

thermophoresis; vesicle trapping; optical tweezers; liposomes; plasmonic heating; optothermal effect

Introduction

A lipid is an amphiphilic molecule, generally with a charged headgroup and a long hydrocarbon tail, of biological origin that is found in the membranes of cells in most lifeforms. The membrane itself is composed of a bilayer of lipids oriented with the lipid hydrocarbon chains interdigitated and a hydrophilic headgroup (which is normally charged) facing outward towards an aqueous environment. Vesicles can serve as models for the membranes of various different organisms based on the type and proportion of lipids, which varies across species, organelle, and biological purpose. In addition, the complex biomolecules found at or in the membrane, including proteins and glycolipids, can be included in vesicle synthesis to study specific aspects of cell interactions and membrane function. Phenomena such as bilayer rupture through the carpet model[1,2], water pore formation[3–5], lipid flip-flop, lipid clustering[6], and lateral diffusion[7] can be studied using vesicles in order to understand specific mechanisms of membrane conformational dynamics and interactions to complement experiments in living cells. In addition, vesicles can be used as containers for the study of enzymatic or other chemical reactions which can be induced by vesicle fusion.[8–10] Numerous sensing strategies have been devised based on the interactions of fluorescently labeled lipids with the external or internal aqueous environment, and release of cargo molecules can be achieved upon analyte binding or in response to stimuli such as UV light.[11] Vesicles have also found applications as drug-delivery systems due to their ability to ferry potentially toxic cargo to specific tissues and biocompatibility which can be controlled by the vesicle composition and surface chemistry.[12–14]

Since the start of the 21st Century, optical tweezers have become a useful tool for the trapping and study of lipid vesicles.[15] While early work found morphological transitions and expulsion of smaller vesicles induced by the laser illumination on the vesicle, numerous studies since have shown its utility for studying phenomena such as dye release[16] and lipid-raft formation[7] and allowing improved Raman and fluorescence spectroscopic measurements.[17,18] Recently, Bendix and Oddershede *et al* have reported a number of interesting studies of optically-trapped vesicles, including the selective fusion of lipid vesicles through hot-nanoparticle mediated fusion.[19–21] The manipulation of organelles inside cells has also been achieved using optical trapping, opening up interesting possibilities for *in situ* studies.[22,23]

Despite the success of optical tweezers in vesicle trapping, there are inherent limitations to particle trapping with optical force. The main limitation with regards to vesicle trapping is the dependence of optical trapping strength on differences in index of refraction, where vesicles have nearly identical refractive indices relative to the surrounding media. In optical trapping, vesicles are typically loaded with a high concentration of a solute such as sucrose

to increase the difference in refractive index between the vesicle and the media. In addition, the experimental setup involved for optical trapping can be quite grueling, requiring rigorous optics and high operational power. Despite some recent advances in optical tweezing techniques[24], attempts to overcome these limitations have been made. Recently plasmonic tweezers, which generate localized plasmonic hot-spots to enhance near-field trapping, have shown promise for optical trapping of nanoparticles while reducing the optical requirements needed.[25–27] Unfortunately, the localization of plasmonic hot spots needed for trapping requires a surface with discrete metal nanostructures, which limits its use to a short-range and does not provide much room for the implementation of dynamic manipulation.[28]

Recently, Lin and coworkers developed a number of novel approaches for trapping and dynamic manipulation based on thermal and electric gradients induced by optical heating on a plasmonic surface, enabling trapping and dynamic manipulation of different colloidal particles as well as cells.[29–32] In response to an applied temperature gradient ∇T, suspended particles are subject to thermophoretic forces and migrate to the cold region (thermophobic) or hot region (thermophilic) with a drift velocity $\boldsymbol{u} = -D_T \nabla T$, where D_T is the thermophoretic mobility. At 0.2 mW, near the upper limit of powers studied herein, thermal gradients of $\nabla T_z = -8.6 \times 10^6$ K/m and $\nabla T_r = -3.6 \times 10^6$ K/m are created at the plasmonic surface in the axial and radial directions, respectively.[31] Through harnessing the thermophilic migration of suspended particles under light-controlled temperature fields, opto-thermophoretic tweezers can potentially overcome the limitations of optical tweezers.[29,33,34] The key to achieve thermophoretic trapping is a negative sign of D_T, where the suspended particles are driven from the cold region to the hot region.

The dominant mechanism of thermophoretic trapping involves the asymmetry of permittivity (ε) at the interface of a lipid bilayer upon encountering a thermal gradient, as discussed in prior work.[29] The interfacial solvent structure plays a significant role in the difference in permittivity of bulk solvent and particle surface. In brief, entropy change in the electric double layer resulting from thermal perturbation of the solvent at the interface of a vesicle can be approximated as $H(z) = \frac{1}{2}(\varepsilon + T\,\partial\varepsilon / \partial T)\,E^2(z)$, where E is a function of the surface potential of the vesicle ζ and the Debye length κ^{-1}described by $E(z) = \kappa\zeta \exp(-\kappa z)$, and z is the distance from the membrane surface (Fig. 1b). In the case of water there tends to be a significant layer of structured water at the particle interface, which in turn leads to a large difference in permittivity, allowing entropy-driven thermophoretic trapping.[35] The thermophoretic drift of molecules, ions, and colloidal particles is directly related to the Soret coefficient S_T, which describes thermophoretic mobility as $S_T = D_T/D$, where D is the Brownian diffusion coefficient. Duhr and Braun have shown that for DNA and polystyrene beads the Soret coefficient is given by the negative solvation entropy divided by kT.[36] However, the Soret coefficient of suspended particles is still not fully understood as it is highly system-specific, exhibiting rich behaviors at different temperatures, surface chemistries, ionic strengths, solute concentrations, *etc*[37]. A recent study by Talbot et al. determined S_T of different pure and mixed lipid vesicles of different compositions, and though the relationship between headgroup chemistry and S_T was established, there was still no correlation found between ζ-potential and S_T even within vesicles of the same lipid type.[38]

The previous study of cell trapping was carried out using both *E. coli* and yeast cells with a size range of 5 – 10 μm, where yeast cell walls are coated with mannoprotein and βglucan and chitin, atop a cell membrane composed largely of neutral lipids with the phosphatidylcholine (PC) headgroup and sterols, and *E.coli* have an anionic outer cell membrane composed primarily of anionic phosphatidylglycerol (PG) and zwitterionic phosphatidylethanolamine (PE) lipids. Despite their differences in surface chemistry, similar trapping was observed for both cell types in the previous study.[31] Opto-thermophoretic trapping of these cells was attributed to the abnormal permittivity gradient due to the adsorption of water molecules on the membrane with specific orientation induced by the temperature gradient, as discussed in the previous paragraph.[29] Vesicles represent small biological particles with a near-negligible refractive index contrast which can be used for both cargo delivery and biophysical studies. Furthermore, their surface chemistry, size, and internal contents can be carefully controlled, something that is generally not possible with actual cells, providing a means to study size and surface chemistry effects on thermophoretic trapping and Soret coefficient.

Herein, anionic PG phospholipid vesicles were prepared and suspended in pure water over a plasmonic substrate, and thermal gradients induced by laser heating on the plasmonic substrate were used for attracting, trapping, and dynamic manipulation of the vesicles (Fig. 1). Zwitterionic and cationic vesicles were also tested and were found to undergo thermophoresis toward the cold region, giving the laser heating spot a repulsive effect (Figure S1). The long-range attraction of vesicles was also demonstrated to lead to a concentrating effect over a radius increasing with optical power, suggesting that this method could find use in miniaturized preconcentrators for lab-on-chip analysis of biogenic vesicles such as exosomes. In addition, the fluorescence spectra and photobleaching of vesicles loaded with the organic dye Rhodamine 101 and CdSe-CdS core-shell quantum dots (QDs) were measured using the heating laser for both trapping and excitation of the fluorophore.

This work presents a novel approach to facile manipulation of lipid vesicles, however the thermophoresis of vesicles toward the hot region is currently only achievable with the anionic lipid DOPG.[38] While the method reported here is a flexible and facile approach to trapping, manipulation, and spectroscopic characterization of trapped anionic liposomes, this is only the first report of opto-thermophoretic trapping, arbitrary control, and large-scale collection of lipid vesicles. Herein we describe the first examples of single-vesicle trapping and manipulation based on thermophoresis, freeing us from the need for a difference in refractive index between the inside and outside of the vesicle as in optical tweezers. In addition, the dual purpose of the low power laser for both thermophoretic trapping and excitation of loaded fluorophores suggest future utility in lab-on-a-chip type analysis. This study sets the stage for extension of this technique to lipids with different headgroup chemistry, control of endogenous lipid bodies such as exosomes, and large-scale collection and separation of different lipid types via tailoring of thermal gradients resulting from optical heating (or cooling) of the substrate. Furthermore, analysis of the effects of plasmonic heating at different powers on vesicle structure reveals the working limitations of the technique and serves as a guide for future research using this approach.

Results and Discussion

Single Vesicle Trapping

Irradiation of a plasmonic surface with a 532 nm laser power of 0.216 mW with a spot size of 2 μm has been previously shown to establish a thermal gradient of $0.5 – 3 \times 10^7$ K m^{-1} with a ~12 K difference between the hot and cold regions.[32] The Soret coefficient S_T, first described by Ludwig and Soret, is a measure of the degree of separation of a species under a thermal gradient, defined by the thermophoretic mobility D_T divided by the diffusion coefficient. [39–41] A 1 μm DOPG vesicle has a Soret coefficient S_T of −0.2 to −0.4 K^{-1} between 20 and 30 00b0C, where DOPC vesicles have a Soret coefficient of ~ 0.2 K^{-1}.[38] It was originally expected that the cationic surface charge of DOTAP vesicles, of which the thermophoretic mobility has not been studied previously, would provide some optothermoelectric field as observed with CTAC micelles and CTAC-coated metal nanoparticles by optothermoelectric nanotweezers.[32] However, the temperature gradient leads to the repulsion of DOTAP vesicles from the laser spot similar to DOPC vesicles (Figure S1). Following this finding, we focused our efforts on the trapping of anionic vesicles composed of DOPG in pure water. As little as 0.1 mM of NaCl strongly reduced thermophoresis of DOPG vesicles in our experiments, and Soret coefficients in general have been shown to be strongly reduced by the presence of ions in solution.[42,43] The strength of trapping was determined by analyzing the variance σ of a trapped vesicle due to Brownian motion while the beam is kept in a fixed position, and can be calculated by $\kappa = (2k_BT)/\sigma^2$, where k_B is Boltzmann's constant, and T is the temperature.[44] An example of the measurement of trapping stiffness can be seen in Figure 2b-d.

In Figure 2b-d we can observe several interesting trends in the trapping stiffness. First, the laser power and trapping stiffness show a strong linear correlation (Fig 2d). It has been previously reported with polystyrene microparticles and noble metal nanoparticles that increased optical power gives an increase in thermophoretic trapping stiffness, a logical finding considering the power directly relates to the magnitude of the thermal gradient. The Soret coefficient of particles increases with particle size, which has been largely attributed to interfacial interactions with the surrounding solvent.[45] Indeed, the interfacial interactions with solvent are deemed to be the primary driving force for thermophoresis[35], and a surface coating or surfactant layer which "unifies" the surface chemistry allowed Braibanti *et al.* to determine that thermophoretic mobility D_T is actually the same across particle sizes. Furthermore, a recent study by Würger demonstrated the size dependence of the Soret coefficient by plotting extant reported data as S_T/r against r to reveal a linear correlation (where r is the radius of the particle).[46] As the Soret coefficient increases with particle size, it is reasonable that we observe increased trapping stiffness with larger vesicle diameters (Figure 2d).[47]

Other than the dependence of Soret coefficient on particle size which largely dictates the trapping stiffness[45,47], the increased trapping stiffness with vesicle size can be attributed to two effects, the hydrodynamic boundary (or near-wall) effect and brownian motion. Assuming that the vesicle-substrate gap is the same for all vesicles, then the larger vesicles experience a larger enhancement of the trapping stiffness due to enhancement of the Soret

coefficient in the vicinity of the hydrodynamic boundary.[46] This effect has also been previously observed by Guan *et al.* in near-field optical tweezers, and thus a similar effect is expected in the present case.[48] Brownian motion of particles is affected by the mass of the particle, where in our case the larger vesicles exhibit less Brownian motion than the smaller ones.[49] This in turn leads to a greater effective trapping stiffness, as the position of the larger vesicles deviates less from the beam center than the smaller ones. Finally, two effects may play a minor role on vesicle trapping. First, as the generation of the thermal gradient occurs at the plasmonic surface, smaller vesicles may experience slightly higher thermal gradients due to their radii being in closer proximity to the surface than the larger vesicles, however in the size range of vesicles studied (1–4 μm), this effect is likely overcome by the other mechanisms stated above. Finally, the scattering force of the laser can lead to trapping, as this is the mechanism employed by optical tweezers. However, at the low powers (<0.5 mW) studied, and with the low refractive index contrast present in our vesicles which have a similar refractive index both inside and out (same media), this effect is negligible.

The trapping stiffnesses measured in this study are within an order of magnitude of those of Bendix and Oddershede, where a 1.2 μm vesicle was trapped with a stiffness of 11.5 pN/μm and an 130 nm vesicle with a stiffness of 3.2 pN/μm.[20] However, the powers needed in their study to achieve trapping of a 1.2 and 0.13 μm vesicles were 170 mW and 850 mW (1064 nm laser), respectively, which is 4–5 orders of magnitude higher optical powers than used herein. Therefore, normalizing for optical power, we are able to achieve stable trapping of a 1 μm vesicle with a stiffness of 805 pN/μm/W (Fig. 2d), compared with a 1.2 μm vesicle in the aforementioned study at 67.6 pN/μm/W, resulting in at least an order of magnitude increased trapping stiffness per unit power. This significantly reduced power enables a much more flexible optical and experimental design, and does not require a refractive index contrast between the vesicle contents and the surrounding medium as in optical tweezers. The simple optical setup also allows control of the heating laser with the microscope stage controls. Furthermore, the use of a digital mirror device (DMD) allows dynamic control of the beam configuration, including shape and number of beams. In Figure 3 examples of vesicle capture, movement, and separation of a single vesicle from a cluster are shown.

A vesicle within a certain radius of the beam, related to the magnitude of the thermal gradient and thus optical power, is drawn to the center of the beam by thermophoresis (Fig. 3a). Once trapped at the beam center with a trapping stiffness related to beam power and vesicle size (Fig. 2a), the vesicle can be moved arbitrary directions and distances at a speed which correlates to the trapping stiffness. Trapping stiffness scales linearly with maximum possible speed of vesicle movement. Finally, turning off the optical heating laser results in the immediate breakdown of the temperature gradient, and subsequently, the permittivity gradient resulting from the difference in solvent structure at the hot and cold sides of the vesicle. This results in the particle being “released”, after which it wanders under the influence of Brownian motion (Figure 3b).

The control of the vesicle using opto-thermophoretic trapping allows arbitrary control over the translation of the vesicle along the plasmonic surface. As an example, a single 0.5 μm vesicle was trapped by one of two beams formed by the DMD, and the two beams were then rotated about the central point equidistant to their initial position. This resulted in the

movement of the 0.5 μm vesicle in a clockwise direction to make a complete circle (Fig. 3b). Also, thermophoresis was used to separate a 2 μm vesicle from a cluster with 3 and 4 μm vesicles (Fig. 3d). Some dragging of the other vesicles in the progress of separation occurred, but the 2 μm vesicle was able to be cleanly separated from the cluster. While this suggests that single vesicle trapping could be complicated by the attraction of other nearby vesicles, the low power used for trapping can largely prevent this. Separation of aggregated vesicles allows manual sorting and identification of the vesicle contents through optical spectroscopy, which is discussed further on.

Multiple Vesicle Trapping and Dynamic Manipulation of Vesicles

While trapping with a single beam can be useful, a controllable multi-beam setup can enable the study of vesicle-vesicle interactions and processes involved in vesicle fusion. In this study, a digital micromirror device (DMD) is used to form arbitrary beam shapes and manipulate them in real time, allowing multi-particle dynamic control. This approach has been successfully used for dynamic manipulation of particles and cells by opto-thermophoresis. In this study, the parallel trapping, controlled movement, and release of DOPG lipid vesicles of different sizes was achieved (Figure 4). Furthermore, parallel trapping was used to bring vesicles near to each other and them pull them apart, which is of great interest for future studies of vesicle interactions.

Snapshots of the approach of two 2.5 μm lipid vesicles is shown by dark-field microscopy in Figure 4a. The vesicles are then separated to their original positions by adjusting the beam locations in real time using the DMD software (Figure 4b). One can observe that there is some adhesion of the vesicles which results in a snapping response when the vesicles are finally separated (between 0 and 0.6 s, Figure 4b, or 45.5 and 45.8 s of Video S3). The ability to dynamically control the spatial relationship between two lipid vesicles enables numerous possible studies related to lipid fusion, biomolecular binding, protein unfolding, controlled drug delivery, and compartmentalized reactors.

Long-range Collection and Concentration of Vesicles

Thermophoresis of particles over long ranges can be achieved, where the velocity is dependent on the size and thermophoretic mobility of the particle. To study the influence of optical heating power on the attraction velocity of vesicles at different distances from the laser spot, vesicles were extruded to a size of 1 μm and the power was varied from 0.27 to 1 mW. Interestingly, large fluctuations in velocity were observed across different vesicles of the same diameter, though the average does show a recognizable trend of higher optical powers leading to both increased velocity overall across a greater distance (Figure 5a,b). The variations in velocity between different vesicles of the same diameter are likely the result of local viscosity changes and changes in the separation distance between the vesicle and the plasmonic surface, both during the attraction to the laser spot and at the start of the measurement. Furthermore, the dependence of the velocity of attracted vesicles on the power of the heating laser can be clearly observed in the difference in collected vesicles between 0.6 and 3 mW, where the former has a cluster of vesicles with a diameter of ~ 4 μm and the latter approaching 15 μm after 30 seconds of irradiation (Figure 5c,d).

Recent studies have shown that opto-thermophoresis can also induce electric field gradients for trapping of gold nanoparticles in surfactant solution, which was originally thought to be a possibility for the mechanism of trapping of vesicles. However, we find that a change of concentration of vesicles does not influence trapping, nor the long-range thermophoretic attraction toward the plasmonic heat spot. Along similar lines, a reduction of vesicle concentration simply results in a slower “supercollection” process, and a correspondingly smaller radius of clustered vesicles at a similar time point. Considering recent interest in the detection of exosomes, a type of biologically-produced liposome which can carry disease markers, the capability to collect vesicles provides a way to package a simple optical “pre-concentrator” for a lab-on-a-chip diagnostic device.

Upper Limits of Optothermal Power

The power of the trapping laser can be increased, effectively enlarging and strengthening the thermal gradient to enable longer-range trapping and eventually either repulsion of a trapped vesicle by high scattering force, or thermally-induced vesicle rupture. We observed that above ~1.3 mW of optical power trapped vesicles are prone to severe structural transitions such as blebbing and rupture, often leading to numerous smaller or multilamellar vesicles (Figure 6, Video S5). Interestingly, in one case a vesicle that was being moved using a laser spot of 1.5 mW was shown to transfer material over several microns distance to a different vesicle, enlarging it (Figure S3).

Considering that the optical power needed for long-range collection of vesicles is much lower (>=0.3 mW), and that trapping requires as little as 11 μW, there is near-zero risk of structural effects or damage to optothermally-trapped vesicles. This is also far below the threshold needed for microbubble formation by up to ~25–35 mW, providing a range of temperatures that such thermal effects can be observed without microbubble formation. The origin of these effects can arise from a range of potential mechanisms, such as strong Marangoni flows, and even explosive fragmentation of the plasmonic metal leading to cavitation and stress-wave generation. Previous studies have shown that under continuous wave illumination, strong Marangoni convection and even micro-bubble formation can occur, which may be strong enough to physically affect the vesicle structure.[50,51] In addition, the instantaneous heating of the plasmonic metal can lead to explosive fragmentation, which is described by cavitation forces and stress-wave generation.[52] While we attribute the physical damage to the vesicles observed herein to strong Marangoni convection, future work using a pulsed-laser source would be needed to disentangle the different possible mechanisms. The powers used to observe the effects resulting from plasmonic heating are well below those reported for optical trapping of lipid vesicles (usually well above >100 mW)[20], suggesting that if these two techniques are to be used in tandem that the wavelength of optical trapping must not overlap with the absorption of the plasmonic component used for optothermal heating. This method may prove useful in future studies of temperature effects on lipid phases, clustering, and vesicle structure. Also, considering the difficulties of observing smaller vesicles and bilayer structures using simple light microscopy, future studies utilizing higher resolution microscopy techniques such as confocal fluorescence microscopy will provide a more detailed view of what is occurring

with the vesicle structure under the temperature gradients produced by the optical heating spot.

In situ Fluorescence Spectroscopy of Fluorophore-Loaded Vesicles

Most experiments involving vesicles utilize spectroscopy of fluorophore-loaded vesicles to study release and diffusion of the fluorophores, or surface-bound fluorophores to monitor morphological dynamics, fusion, and binding interactions of the vesicles. In a simple fluorescence microscope, one would typically use a broadband light source such as a halogen lamp in conjunction with a set of filter cubes designed for typical fluorophores, such as fluorescein isothiocyanate (FITC), Rhodamine, and 4',6-diamidino-2-phenylindole (DAPI). The spectra obtained using this method can be sub-optimal due to a low fluorescence intensity leading to high signal to noise, as well as the different filters in the cube needed for excitation blocking spectral acquisition outside of the range of 575 to 650 nm (Figure 7a). However, the use of the trapping laser to excite the fluorophore allows the acquisition of the entire spectral range, as no filter cube is needed (Figure 7b). Furthermore, the excitation of the vesicle under the laser provides less exposure of the surrounding medium, leading to a higher signal to noise ratio. The fluorescence spectroscopy of trapped vesicles containing these two fluorophores demonstrated that dual use of the optical heating laser as an excitation source can be used to give improved spectroscopic measurements compared to the traditional lamp-cube combination (Figure 7).

We observe that while the CdSe-CdS fluorescence is consistent with some sharp variations in intensity that are likely due to photoblinking (Figure 7c), the fluorescence of Rhodamine 101 is clearly shown to photobleach over 2 minutes (Figure 7d). It would be difficult to use the same trapping-excitation scheme with optical tweezers, as their high optical power would lead to more rapid photobleaching and very high fluorescence intensities that could damage the photodetector. However, it should be noted that the surface chemistry of the vesicle resulting from the anionic lipid headgroups dictates the thermophoretic mobility, and excessive free dye in the medium could disrupt this chemistry and lead to a positive S_T. This is complicated by the fact that each molecular, nanoparticulate, or macromolecular guest will have its own Soret coefficient and that determination of their interactions will have to be performed on a case by case basis.

Conclusions

Phospholipid vesicles are widely used as sensors, drug-delivery vehicles, nanocontainers for reactions, and membrane mimetics to study biophysical processes, in which their importance for future studies of virulence, protein misfolding, and cellular signaling processes cannot be overstated. Herein, thermophoretic trapping of anionic lipid vesicles composed of DOPG was achieved through optical heating of a plasmonic substrate, providing a unique approach to manipulation of single vesicles. The opto-thermophoretic trapping method overcomes some of the limitations of traditional optical tweezers, namely rigorous optical component setup and high optical power, while providing an increase in trapping stiffness with lower power needs. Another major advantage of opto-thermophoretic trapping is that particles with a refractive index similar to the refractive index of the environment are trapped, whereas in

traditional optical tweezers the trapping stiffness increases with the ratio of the refractive index of the particle to that of the medium. A typical strategy to enable traditional optical trapping of vesicles involves loading the vesicle with a high concentration of sucrose (2M) to achieve an increased refractive index compared to the surrounding medium.[20] Opto-thermophoretic trapping overcomes this limitation, allowing trapping of particles with the same refractive index as the surrounding medium. Despite significant recent advances in vesicle manipulation enabled by optical tweezers,[53] this technique provides a means for low-power trapping of vesicles with a similar refractive index as water.

The single-vesicle trapping shown herein fills the gap between prior studies of opto-thermophoretic trapping of different cell types and bulk studies of thermophoresis of lipid vesicles. In the previous study of cell trapping, both *E. coli* and yeast cells of ~ 5–10 μm were able to be trapped despite their clear differences in surface chemistry.[31] The use of vesicles allows control over both the size and surface chemistry, which can then in turn lead to greater information about how the individual components of the vesicle influence the trapping of cells, which have a complex mixture of lipids in their cell membrane in addition to diverse other biomolecules depending on the organism. Furthermore, this study sheds light on some of the potential applications of vesicle thermophoresis. Vesicles can be attracted over large distances (up to hundreds of microns) to the laser spot, which can be useful for preconcentration of vesicles for lab-on-chip spectroscopic detection of cargo. This is quite useful considering that exosomes, vesicles produced by cells, contain useful biomarkers for disease and particularly cancer diagnosis, and state-of-the-art methods such as centrifugation and field-flow fractionation are not nearly as simple.[54] Recent studies have shown that that thermal mixing could induce the aggregation of lipid vesicles using gold nanoparticles, however this involves the suspension of vesicles with nanoparticles, which can interact strongly with and disrupt the lipid bilayer.[55]

A further benefit, vesicle trapping was shown to be a means to hold vesicles containing fluorophores in place for fluorescence spectroscopic measurements. Comparing with the traditional combination of lamp and fluorescence filter cube, the optical heating laser was used for both trapping and excitation of the loaded fluorophores. This approach enabled spectroscopic monitoring of vesicle-loaded QDs and organic dyes, where photobleaching of the latter was clearly observed. Spectroscopic measurements on sensitive organic fluorophores which have an absorption band in the region of the trapping laser are a challenge for traditional optical tweezers, while the low optical power needed for thermophoretic trapping makes it possible. Finally, dynamic and parallel trapping carried out with the aid of a digital mirror device (DMD) provided a means for arbitrary control of vesicle position and control over vesicle-vesicle interactions, which is crucial for studies of vesicle binding by molecules incorporated into the membrane.

While opto-thermophoretic control can facilitate experimental observation of changes in lipid phase behavior upon heating to the lipid transition temperature T_m, we opted to use DOPG as it has a T_m below freezing and allowed us to study thermophoretic trapping and manipulation without confounding effects from plasmonic heating induced lipid phase transitions. However, phase changes preceding rupture such as blebbing were observed at higher optical powers (>1.5 mW), suggesting that this method could be used at higher power

regimes for studying thermophysical changes in membrane structure. Using simple light microscopy it was not possible to truly quantitate the blebbing or bursting behavior due to the inability to observe very small membrane structures, and therefore observations of the initial phase changes and small structural deformations of the vesicle may require the use of confocal fluorescence microscopy or other higher resolution microscopy.

While the thermophoretic mobility of different colloidal particles is system-specific and not yet fully understood, the future of thermophoretic trapping for control of biological systems and in vitro studies of biological processes is bright. Furthermore, the results reported herein were obtained using a simple light microscope, suggesting that future studies with higher resolution microscopy techniques will yield additional exciting observations. Finally, this method provides an additional tool which can complement optical tweezers to allow both manipulations using thermal gradients and optical scattering forces. The combination of optical tweezers and optically-generated thermal gradients presents an interesting way to study fluctuations in mixed lipid vesicles, lipid rafts, and thermophysical effects on optically-trapped lipid vesicles. We look forward to the continuation of developments in this field and resulting advances in life sciences.

Methods

Materials

1,2-dioleoyl-sn-glycero-3-phospho-(1’-rac-glycerol) (DOPG) sodium salt, 1,2-dioleoyl-3trimethylammonium-propane (DOTAP) chloride salt, and 1,2-dioleoyl-sn-glycero-3phosphocholine (DOPC) powders, obtained from Avanti Polar Lipids, were dissolved in CH_3Cl (50 mg/2.5 mL) in brown glass vials with Teflon-coated caps, and stored under N_2 atmosphere at −2000b0C. PEG-functionalized Core-shell CdSe-CdS quantum dots with emission at 590 nm in aqueous solution (4 μM) were obtained from a collaborator. Rhodamine 101 inner salt was obtained from Acros Organics. The AuNP substrate was fabricated by depositing a 4 nm Au thin film on a glass slide with thermal deposition (Denton thermal evaporator; base pressure, 1×10−5 Torr) followed by thermal annealing at 550 °C for 2 h. The thickness of the Au film was chosen to enable a high absorption efficiency (~50%) at the laser wavelength of 532 nm.[29]

Vesicle Preparation

Large unilamellar vesicles of different sizes were prepared as follows: 100 μL of a lipid solution in chloroform (20 mg/mL) was deposited into a glass vial, dried under N_2 for 10 min, and placed under vacuum for 2 h. Second, the lipid film was rehydrated with 4 ml of N_2-degassed water (resistivity of 18.2 MΩ-cm), and stirred with a magnetic stirbar at 1100 rpm for 1 hr. Some vesicles were then extruded with atleast 15 passes through a 1.0 μm membrane. The vesicles were stored at 400b0C and used within a week. Dynamic light scattering and ζ-potential measurements were taken using a Malvern Zetasizer Nano ZS. The DOPG vesicles formed by this approach consist of a ζ-potential of −40.6 +/− 13.0 mV and hydrodynamic radii mostly in the range of1–10 μm (Figure S2). This suspension was diluted in water for further experiments, and the final concentration of lipids in a sample was 0.05 – 0.01 mg/mL. In the preparation of QDloaded and Rhodamine 101-loaded vesicles, to

the 4 mL of water used to suspend the dry lipid film was added 200 μL of CdSe – CdS core-shell nanoparticles functionalized with Poly(maleic anhydride-alt-1-octadecene) – Polyethylene glycol (4 μM)[56], and 4 μL of Rhodamine 101 (2 mM), respectively. We chose CdSe-CdS core-shell quantum dots (λ_{em} = 491 nm) and Rhodamine 101 since one serves as a model for a colloidal nanoparticle suspension and one as a typical organic dye.

Optical setup

A 532 nm laser beam (Coherent, Genesis MX STM-1 W) was expanded to a diameter of ~ 5 mm with a beam expander (Thorlabs, GBE05-A) and projected onto a computer-controlled DMD to allow customization of the beam shape. The optical images reflected from the DMD were relayed onto the substrate through a 1000 mm doublet lens, a 200 mm doublet lens, an infinity-corrected tube lens, and a 40× objective lens (Nikon, NA 0.75) in an inverted optical microscope (Nikon Ti-E). The DMD and lens were removed from the setup and a 100X oil lens (Nikon, NA 0.7–1.3) was used when measuring the trapping stiffness in Fig. 3. Real-time optical imaging was achieved using a color CCD (Nikon) and the particle tracking was achieved using a fast monochromic CCD (Andor). A 533 nm notch filter was inserted between the objective and the camera to block the laser beam. The beam power impinging on the sample was measured using a Thorlabs PM-100D power meter.

Trapping Stiffness Measurements

The strength of trapping is determined by analyzing the variance σ of a trapped vesicle due to Brownian motion while the beam is kept in a fixed position, calculated by $\kappa = (2k_BT)/\sigma^2$. The position of the vesicle in one dimension while trapped is fit to a gaussian distribution, giving the variance (Fig. 2c). Measurements were an average of multiple vesicles (n>5) per size, and were also an average of the stiffness in the X and Y directions.

Fluorescence Measurements

Fluorescence spectra of trapped vesicles were taken using an Andor Shamrock 303i spectrograph (grating: 299 l/mm and slit width: 50 μm) and a Newton EMCCD integrated with an inverted Nikon microscope. The background signal was subtracted from the fluorescence spectra. The 532 nm laser was used for both trapping and excitation of the QDs with 0.11 mW power. A 0.1-second acquisition time was used for kinetics and a 3 second acquisition time was used for spectra. In a traditional approach to measuring the fluorescence using a white light source and a filter cube, a 660 nm DPSS laser (Laser Quantum, OPS 1500, 1.5 W) was used for trapping the Rhodamine 101-loaded vesicles using a 5× beam expander and focused onto the plasmonic substrate with a 40× objective (Nikon, NA 0.75) in an inverted microscope. Background spectra were taken of the plasmonic substrate at least 100 μm from any vesicle under lamp and laser illumination conditions of those used for trapping and spectral acquisition.

Supplementary Material

Refer to Web version on PubMed Central for supplementary material.

Acknowledgements

We acknowledge the financial support of the Beckman Young Investigator Program, the Army Research Office (W911NF-17–1-0561), the National Aeronautics and Space Administration Early Career Faculty Award (80NSSC17K0520) and the National Institute of General Medical Sciences of the National Institutes of Health (DP2GM128446). E.H.H. acknowledges support by the German Academic Exchange Service (DAAD), from funds of the German Federal Ministry of Education and Research (BMBF) (57429511). We thank Dr. William W. Yu for providing the quantum dots.

References

(1). Wang Y; Tang Y; Zhou Z; Ji E; Lopez GP; Chi EY; Schanze KS; Whitten DG Membrane Perturbation Activity of Cationic Phenylene Ethynylene Oligomers and Polymers: Selectivity against Model Bacterial and Mammalian Membranes. Langmuir 2010, 26 (15), 12509–12514. [PubMed: 20586429]

(2). Hill EH; Whitten DG; Evans DG A Computational Study of Bacterial Membrane Disruption by Cationic Biocides: Structural Basis for Water Pore Formation A Computational Study of Bacterial Membrane Disruption by Cationic Biocides: Structural Basis for Water Pore Formation. 2014.

(3). Woo H-J; Wallqvist A Spontaneous Buckling of Lipid Bilayer and Vesicle Budding Induced by Antimicrobial Peptide Magainin 2: A Coarse-Grained Simulation Study. J. Phys. Chem. B 2011, 115 (25), 8122–8129. [PubMed: 21651300]

(4). Hill EH; Stratton K; Whitten DG; Evans DG Molecular Dynamics Simulation Study of the Interaction of Cationic Biocides with Lipid Bilayers: Aggregation E Ff Ects and Bilayer Damage. 2012.

(5). Ros U; García-Sáez AJ More Than a Pore: The Interplay of Pore-Forming Proteins and Lipid Membranes. J. Membr. Biol 2015, 545–561. [PubMed: 26087906]

(6). Wadhwani P; Epand RF; Heidenreich N; Bürck J; Ulrich, a S.; Epand, R. M. Membrane-Active Peptides and the Clustering of Anionic Lipids. Biophys. J 2012, 103 (2), 265–274. [PubMed: 22853904]

(7). Collard L; Perez-Guaita D; Faraj BHA; Wood BR; Wallis R; Andrew PW; Hudson AJ Light Scattering by Optically-Trapped Vesicles Affords Unprecedented Temporal Resolution of Lipid-Raft Dynamics. Sci. Rep 2017, 7 (1), 1–11. [PubMed: 28127051]

(8). Wang X; Feng J; Bai Y; Zhang Q; Yin Y Synthesis, Properties, and Applications of Hollow Micro-/Nanostructures. Chem. Rev 2016, 116 (18), 10983–11060. [PubMed: 27156483]

(9). Trantidou T; Friddin M; Elani Y; Brooks NJ; Law RV; Seddon JM; Ces O Engineering Compartmentalized Biomimetic Micro- and Nanocontainers. ACS Nano 2017, 11 (7), 6549–6565. [PubMed: 28658575]

(10). Bolinger PY; Stamou D; Vogel H Integrated Nanoreactor Systems: Triggering the Release and Mixing of Compounds inside Single Vesicles. J. Am. Chem. Soc 2004, 126 (28), 8594–8595. [PubMed: 15250679]

(11). Edwards KA; Baeumner AJ Liposomes in Analyses. Talanta 2006, 68 (5), 1421–1431. [PubMed: 18970481]

(12). Samad A; Sultana Y; Aqil M Liposomal Drug Delivery Systems: An Update Review. Curr. Drug Deliv 2007, 4 (4), 297–305. [PubMed: 17979650]

(13). Lee J; Kim J; Jeong M; Lee H; Goh U; Kim H; Kim B; Park JH Liposome-Based Engineering of Cells to Package Hydrophobic Compounds in Membrane Vesicles for Tumor Penetration. Nano Lett. 2015, 15 (5), 2938–2944. [PubMed: 25806671]

(14). Kraft JC; Freeling JP; Wang Z; Ho RJY Emerging Research and Clinical Development Trends of Liposome and Lipid Nanoparticle Drug Delivery Systems. J. Pharm. Sci 2014, 103 (1), 29–52. [PubMed: 24338748]

(15). Vasdekis AE; Scott EA; Roke S; Hubbell JA; Psaltis D Vesicle Photonics. Annu. Rev. Mater. Res 2013, 43 (1), 283–305.

(16). Schaefer JJ; Ma C; Harris JM Confocal Raman Microscopy Probing of TemperatureControlled Release from Individual, Optically-Trapped Phospholipid Vesicles. Anal. Chem 2012, 84 (21), 9505–9512. [PubMed: 23043532]

(17). Cherney DP; Conboy JC; Harris JM Optical-Trapping Raman Microscopy Detection of Single Unilamellar Lipid Vesicles. Anal. Chem 2003, 75 (23), 6621–6628. [PubMed: 14640737]

(18). Hashemi Shabestari M; Meijering AEC; Roos WH; Wuite GJL; Peterman EJG Recent Advances in Biological Single-Molecule Applications of Optical Tweezers and Fluorescence Microscopy, 1st ed.; Elsevier Inc., 2017; Vol. 582.

(19). Rørvig-Lund A; Bahadori A; Semsey S; Bendix PM; Oddershede LB Vesicle Fusion Triggered by Optically Heated Gold Nanoparticles. Nano Lett. 2015, 15 (6), 4183–4188. [PubMed: 26010468]

(20). Bendix PM; Oddershede LB Expanding the Optical Trapping Range of Lipid Vesicles to the Nanoscale. Nano Lett. 2011, 11 (12), 5431–5437. [PubMed: 22074221]

(21). Bahadori A; Moreno-Pescador G; Oddershede LB; Bendix PM Remotely Controlled Fusion of Selected Vesicles and Living Cells: A Key Issue Review. Reports Prog. Phys 2018, 81 (3), 032602.

(22). Norregaard K; Metzler R; Ritter CM; Berg-Sørensen K; Oddershede LB Manipulation and Motion of Organelles and Single Molecules in Living Cells. Chem. Rev 2017, 117 (5), 4342–4375. [PubMed: 28156096]

(23). Sacconi L; Tolić-Nørrelykke IM; Stringari C; Antolini R; Pavone FS Optical Micromanipulations inside Yeast Cells. Appl. Opt 2005, 44 (11), 2001–2007. [PubMed: 15835347]

(24). Ott D; Nader S; Reihani S; Oddershede LB Simultaneous Three-Dimensional Tracking of Individual Signals from Multi-Trap Optical Tweezers Using Fast and Accurate Photodiode Detection. Opt. Express 2014, 22 (19), 23661. [PubMed: 25321832]

(25). Huft PR; Kolbow JD; Thweatt JT; Lindquist NC Holographic Plasmonic Nanotweezers for Dynamic Trapping and Manipulation. Nano Lett. 2017, 17 (12), 7920–7925. [PubMed: 29144755]

(26). Juan ML; Righini M; Quidant R Plasmon Nano-Optical Tweezers. Nat. Photonics 2011, 5 (6), 349–356.

(27). Righini M; Zelenina A; Quidant R Parallel and Selective Trapping in a Patterned Plasmonic Landscape. 2007 IEEE/LEOS Int. Conf. Opt. MEMS Nanophotonics, OMENS 2007, 61–62.

(28). Ndukaife JC; Kildishev AV; Nnanna AGA; Shalaev VM; Wereley ST; Boltasseva A Long-Range and Rapid Transport of Individual Nano-Objects by a Hybrid Electrothermoplasmonic Nanotweezer. Nat. Nanotechnol 2016, 11 (1), 53–59. [PubMed: 26524398]

(29). Lin L; Peng X; Mao Z; Wei X; Xie C; Zheng Y Interfacial-Entropy-Driven Thermophoretic Tweezers. Lab Chip 2017, 17, 3061–3070. [PubMed: 28805878]

(30). Lin L; Zhang J; Peng X; Wu Z; Coughlan ACH; Mao Z; Bevan MA; Zheng Y Opto-Thermophoretic Assembly of Colloidal Matter. Sci. Adv 2017, 3 (9), 1–10.

(31). Lin L; Peng X; Wei X; Mao Z; Xie C; Zheng Y Thermophoretic Tweezers for Low-Power and Versatile Manipulation of Biological Cells. ACS Nano 2017, 11 (3), 3147–3154. [PubMed: 28230355]

(32). Lin L; Wang M; Peng X; Lissek EN; Mao Z; Scarabelli L; Adkins E; Coskun S; Unalan HE; Korgel BA; et al. Opto-Thermoelectric Nanotweezers. Nat. Photonics 2018.

(33). Fukuyama T; Fuke A; Mochizuki M; Kamei KI; Maeda YT Directing and Boosting of Cell Migration by the Entropic Force Gradient in Polymer Solution. Langmuir 2015, 31 (46), 12567–12572. [PubMed: 26496637]

(34). Jiang HR; Wada H; Yoshinaga N; Sano M Manipulation of Colloids by a Nonequilibrium Depletion Force in a Temperature Gradient. Phys. Rev. Lett 2009, 102 (20), 1–5.

(35). Peng X; Lin L; Hill EH; Kunal P; Humphrey S; Zheng Y Opto-Thermophoretic Manipulation of Colloidal Particles in Non-Ionic Liquids. 2018, submitted.

(36). Duhr S; Braun D Why Molecules Move along a Temperature Gradient. Proc. Natl. Acad. Sci 2006, 103 (52), 19678–19682. [PubMed: 17164337]

(37). Piazza R; Parola A Thermophoresis in Colloidal Suspensions. J. Phys. Condens. Matter 2008, 20 (15).

(38). Talbot EL; Kotar J; Parolini L; Di Michele L; Cicuta P Thermophoretic Migration of Vesicles Depends on Mean Temperature and Head Group Chemistry. Nat. Commun 2017, 8 (May), 1–8. [PubMed: 28232747]

(39). Ludwig C Diffusion Zwischen Ungleich Erwärmten Orten Gleich Zusammengesetzter Lösung. Sitz. ber. Akad. Wiss. Wien Math.-Nat. wiss. Kl 1856, 20, 539.

(40). Soret C. Arch. Genève 1879, 3, 48.

(41). Wiegand S Thermal Diffusion in Liquid Mixtures and Polymer Solutions. J. Phys. Condens. Matter 2004, 16 (10), 357–379.

(42). Würger A Thermal Non-Equilibrium Transport in Colloids. Reports Prog. Phys 2010, 73 (12).

(43). Piazza R Thermophoresis: Moving Particles with Thermal Gradients. Soft Matter 2008, 4 (9), 1740–1744.

(44). Florin E-L; Pralle a.; Stelzer EHK; Hörber JKH Photonic Force Microscope Calibration by Thermal Noise Analysis. Appl. Phys. A Mater. Sci. Process 1998, 66 (7), S75–S78.

(45). Braibanti M; Vigolo D; Piazza R Does Thermophoretic Mobility Depend on Particle Size? Phys. Rev. Lett 2008, 100 (10), 1–4.

(46). Würger A Hydrodynamic Boundary Effects on Thermophoresis of Confined Colloids. Phys. Rev. Lett 2016, 116 (13), 1–5.

(47). Putnam SA; Cahill DG; Wong GCL Temperature Dependence of Thermodiffusion in Aqueous Suspensions of Charged Nanoparticles. Langmuir 2007, 23 (18), 9221–9228. [PubMed: 17655335]

(48). Guan D; Hang ZH; Marcet Z; Liu H; Kravchenko II; Chan CT; Chan HB; Tong P Direct Measurement of Optical Force Induced by Near-Field Plasmonic Cavity Using Dynamic Mode AFM. Sci. Rep 2015, 5 (October), 1–12.

(49). Lemons DS; Gythiel A Paul Langevin's 1908 Paper "On the Theory of Brownian Motion" ["Sur La Théorie Du Mouvement Brownien," C. R. Acad. Sci. (Paris) 146, 530–533 (1908)]. Am. J. Phys 1997, 65 (11), 1079–1081.

(50). Baffou G; Polleux J; Rigneault H; Monneret S Super-Heating and Micro-Bubble Generation around Plasmonic Nanoparticles under Cw Illumination. J. Phys. Chem. C 2014, 118 (9), 4890–4898.

(51). Baffou G; Quidant R Thermo-Plasmonics: Using Metallic Nanostructures as Nano-Sources of Heat. Laser & Photonics Rev. 2013, 7 (2), 171–187.

(52). Hashimoto S; Werner D; Uwada T Studies on the Interaction of Pulsed Lasers with Plasmonic Gold Nanoparticles toward Light Manipulation, Heat Management, and Nanofabrication. J. Photochem. Photobiol. C Photochem. Rev 2012, 13 (1), 28–54.

(53). Bolognesi G; Friddin MS; Ces O; Elani Y; Salehi-reyhani A; Barlow NE; Brooks NJ Sculpting and Fusing Biomimetic Vesicle Networks Using Optical Tweezers. Nat. Commun 2018, ASAP.

(54). Peinado H; Alečković M; Lavotshkin S; Matei I; Costa-Silva B; Moreno-Bueno G; HerguetaRedondo M; Williams C; García-Santos G; Ghajar CM; et al. Melanoma Exosomes Educate Bone Marrow Progenitor Cells toward a Pro-Metastatic Phenotype through MET. Nat. Med 2012, 18, 883. [PubMed: 22635005]

(55). Kuboi M; Takeyasu N; Kaneta T Enhanced Optical Collection of Micro- and Nanovesicles in the Presence of Gold Nanoparticles. 2018.

(56). Yu WW; Chang E; Falkner JC; Zhang J; Al-Somali a M.; Sayes CM; Johns J; Drezek R; Colvin VL Forming Biocompatible and Nonaggregated Nanocrystals in Water Using Amphiphilic Polymers. J. Am. Chem. Soc 2007, 129 (10), 2871–2879. [PubMed: 17309256]

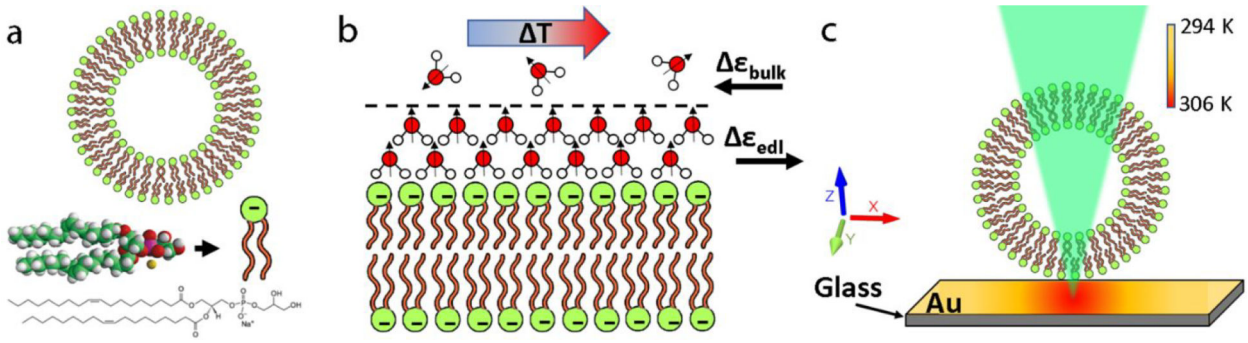

Figure 1.

a) Structure of DOPG and schematic of lipid and vesicle; b) Solvent ordering at the interface leads to a different permittivity at the electric double layer; c) A schematic of the resulting trapping of vesicle at the hot region of the temperature gradient with sodium ions toward the cold region.

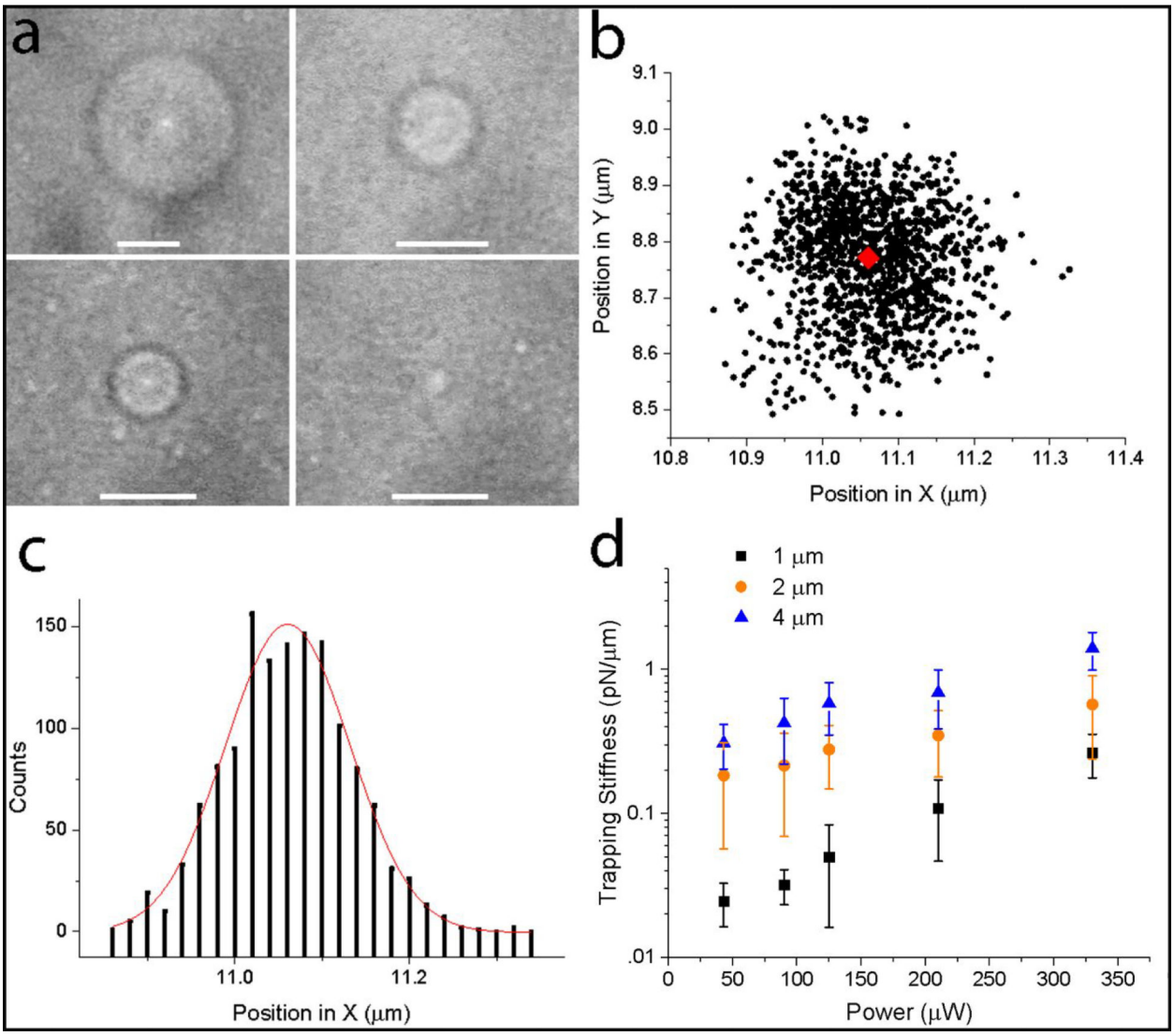

Figure 2.

a) Trapping of different sized DOPG vesicles viewed under bright-field microscopy, scale bars are 5 μm; b) Scatterplot of 2 μm vesicle position in X measured over 10 seconds while trapped with an optical power of 110 μW, the laser spot is indicated by the red diamond; c) Histogram and gaussian fit of frequency distribution of positions measured along the X axis in (b); d) Thermophoretic trapping stiffness of vesicles of different size with varying optical power of the heating laser.

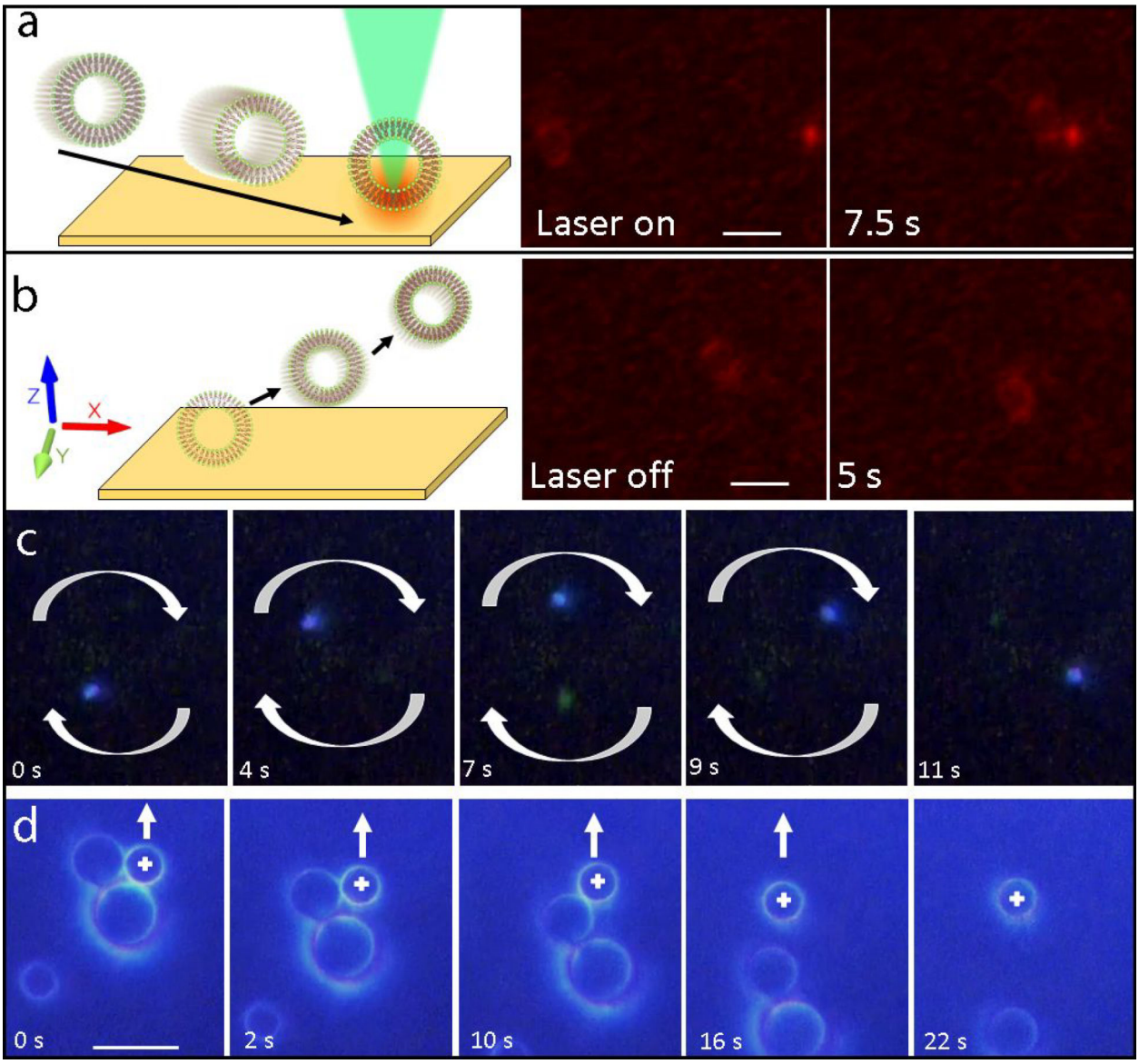

Figure 3.

Dark-field microscopy of single vesicle trapping using opto-thermophoretic trapping: Approach of a vesicle to the laser spot, indicated with the white cross (a); following trapping, the laser is turned off and the vesicle meanders via Brownian motion.(b); Circular movement of a single 0.5 μm vesicle (blue) using rotating beam spots (c); the white arrows indicate the clockwise rotation of the two beams (Video S1); Separation of a single 2 μm vesicle from a three vesicle cluster (d); the white + sign indicates the beam position, and the white arrow indicates the direction of movement following the snapshot (Video S2). Scale bars are 5 μm.

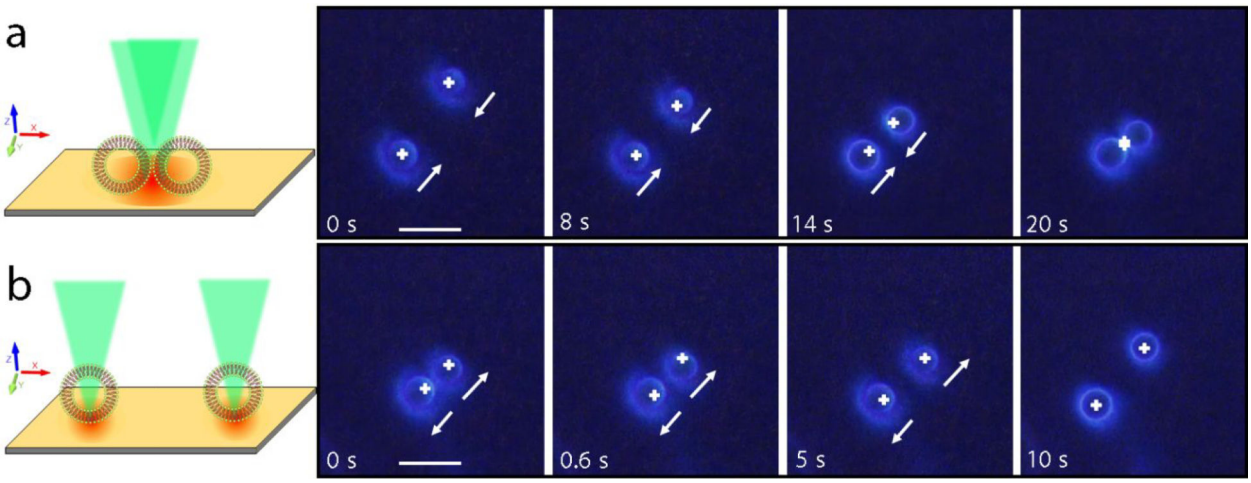

Figure 4.

Dynamic two-vesicle manipulation using DMD-controlled beams. The schematics on the left of the video snapshots represent the final frame of each series. Two 2.5 μm DOPG vesicles are brought into close contact over 20 s (a). They are trapped in contact with one another for an additional 30 s. They are then separated over 10s by moving the beams along a similar trajectory in reverse (b). Beam positions are marked by a white + symbol and a white circle in the case of the 1 μm vesicle, and the direction of movement following the current frame is given by a white arrow. Scale bars are 5 μm.

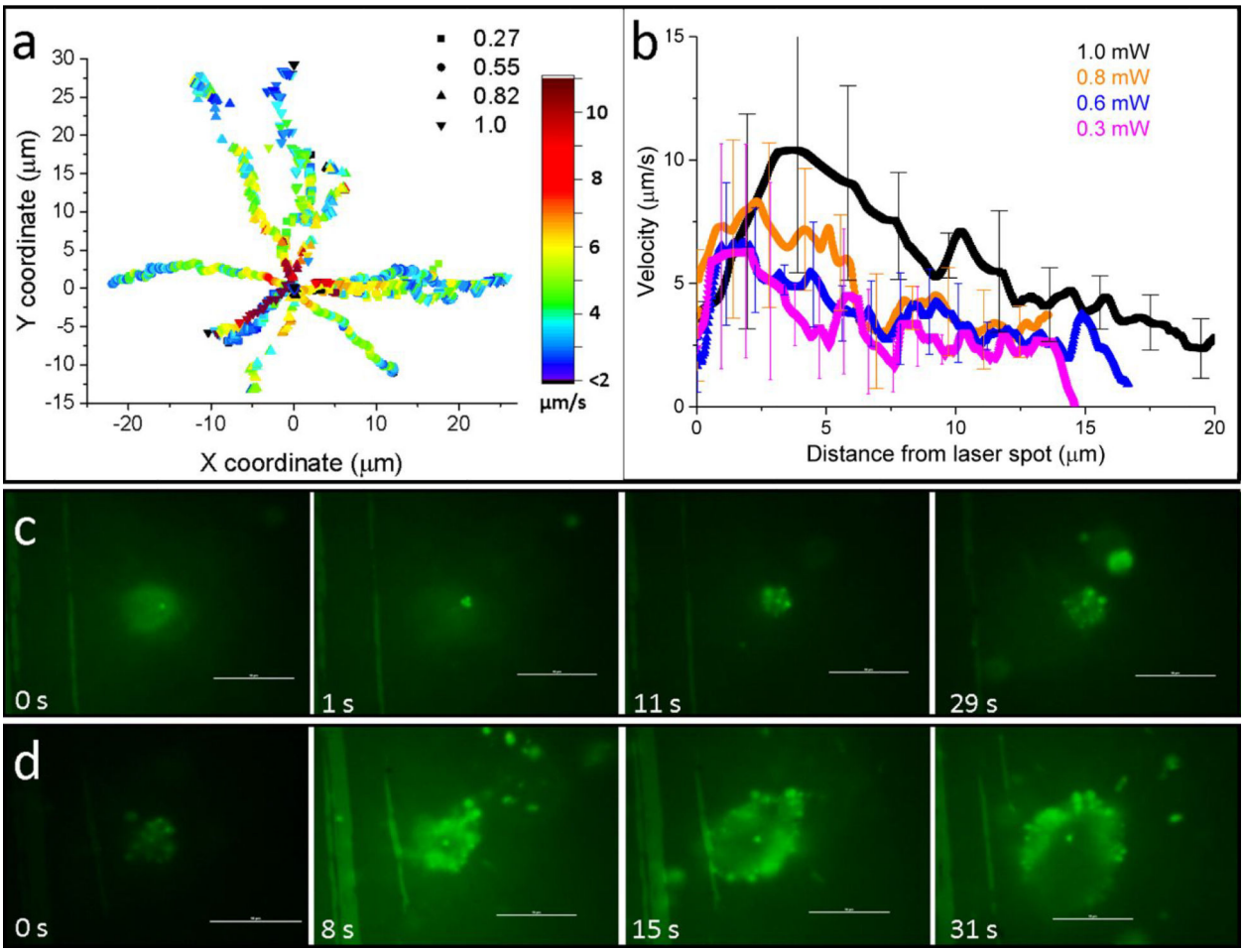

Figure 5.

Long-range attraction and collection of DOPG vesicles at the laser spot. (a) Motion tracks of 1 um vesicles at different optical powers, with velocity shown. (b) Average vesicle velocity as a function of distance from the laser spot. (c) R6G-loaded vesicle collection using a 0.6 mW beam (Video S4). (d) Collection using a 3 mW beam, with photobleaching of vesicles occurring surrounding the beam spot. Scale bars in c and d are 10 μm.

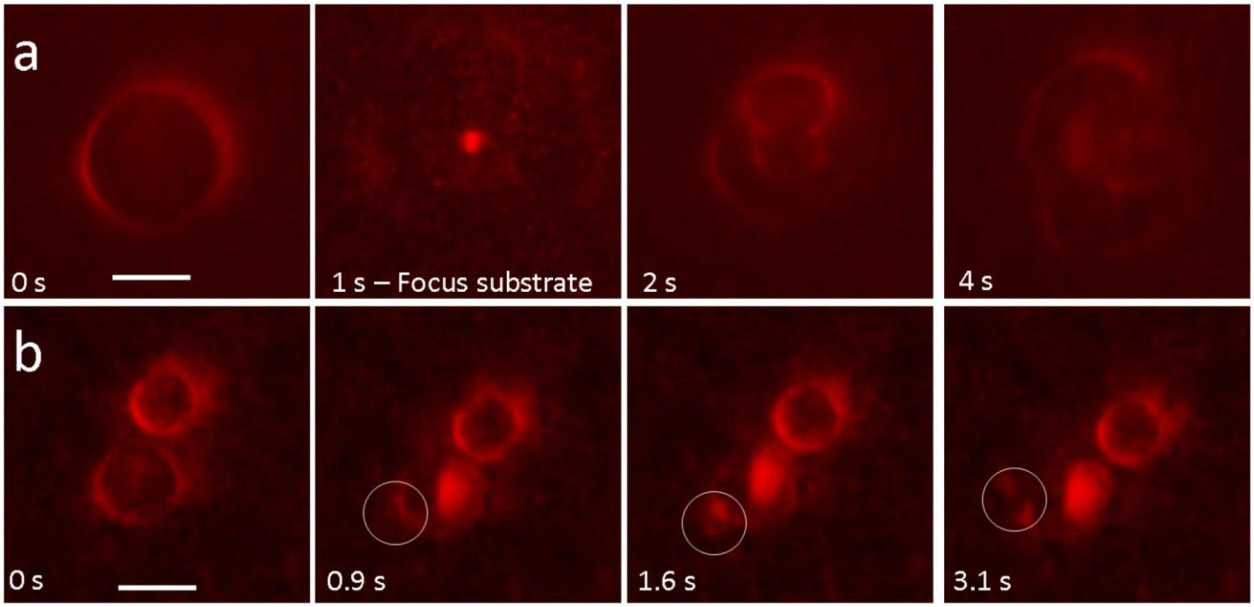

Figure 6.

Deleterious effects of high optical heating power on vesicle structure. 1.3 mW irradiation leads to vesicle rupture and formation of smaller vesicles from a 15 μm vesicle (Video S5) (a). Clear evidence of blebbing of a 10 μm vesicle is shown in the white circles (b). The scale bar is 10 μm.

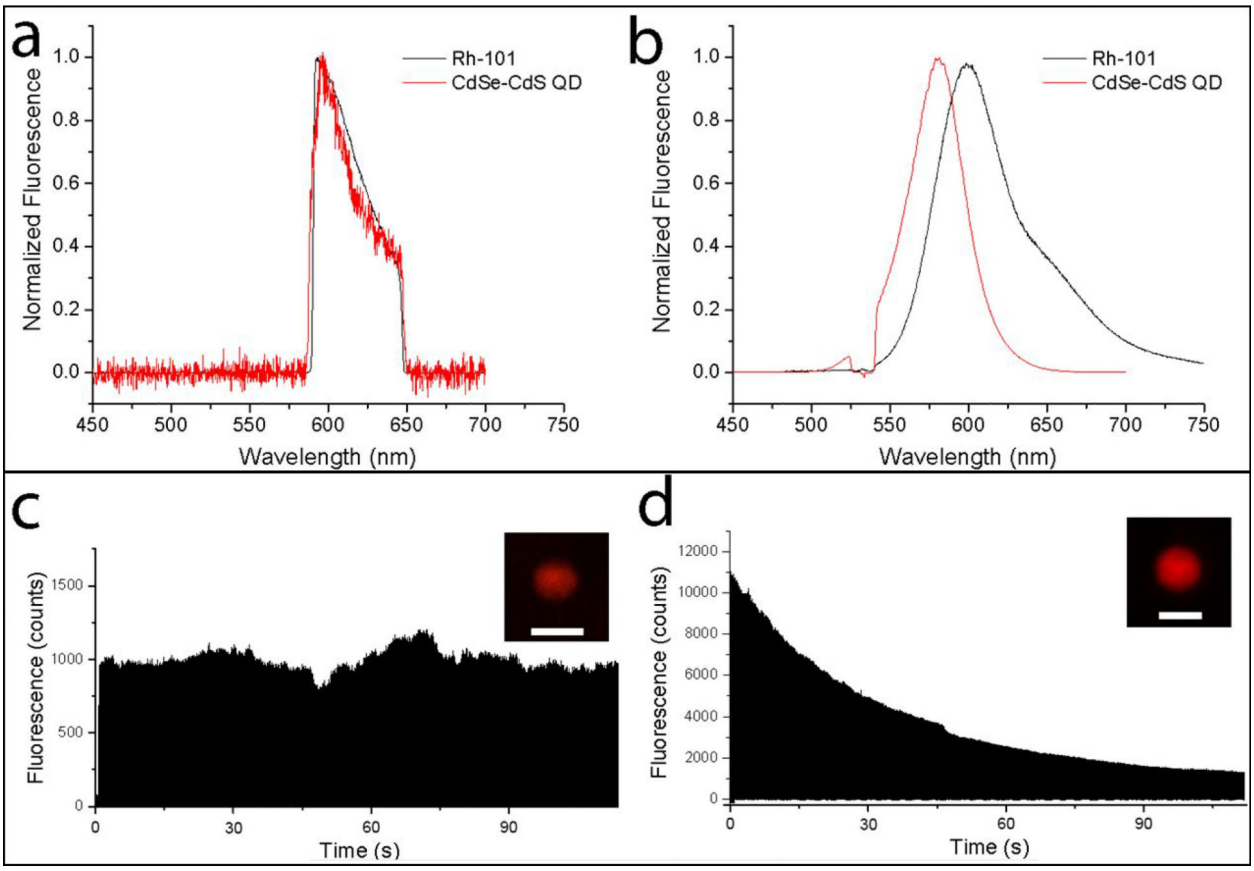

Figure 7.

Fluorescence spectra of vesicles loaded with Rhodamine 101 and CdSe-CdS QDs, excited with a Halogen lamp using a TRITC filter cube (a), and with a 532 nm trapping laser at 0.11 mW (b). Fluorescence of a trapped 4 μm vesicle loaded with 0.2 μM QDs excited with 0.11 mW at 532 nm (c), and with 2 μM Rhodamine-101 excited with 63 μW at 532 nm. Dark-field fluorescence microscopy images are shown as insets in (c) and (d), where scale bars are 5 μm.